Icarus **137**, 260–268 (1999)
Article ID icar.1999.6047, available online at http://www.idealibrary.com on IDEAL®

Imaging Observations of Asteroids with Hubble Space Telescope

Alex Storrs

Space Telescope Science Institute, 3700 San Martin Drive, Baltimore, Maryland 21218
E-mail: storrs@stsci.edu

Ben Weiss

Amherst College, Amherst, Massachusetts

Ben Zellner

Georgia Southern University, Statesboro, Georgia

Win Burleson

Rice University, Houston, Texas

Rukmini Sichitiu

Dartmouth College, Hanover, New Hampshire

Eddie Wells and Charles Kowal

Computer Sciences Corporation, STScI, Baltimore, Maryland

and

David Tholen

Institute for Astronomy, University of Hawaii, Honolulu, Hawaii

Received April 23, 1998; revised September 8, 1998

We present the results of two Hubble Space Telescope (HST) observing programs, consisting of 11 imaging observations of 10 asteroids. The primary focus of the projects was to search for faint companions (satellites) of these asteroids. No binary systems were detected. More specifically, no companions were found at more than 0.1 arcsec separation of brightness down to 4 magnitudes fainter than the primary asteroid. No companions down to 6 magnitudes fainter than the primary asteroid were found at more than 0.5 arcsec separation. It is unlikely that companions more than 6 magnitudes fainter than a well-exposed primary would be detected. These nondetections place very stringent limits on the existence of companion bodies for these asteroids. A secondary goal was to resolve the illuminated portion of the asteroids. Nine of the 10 asteroids were marginally resolved, with three of these—9 Metis, 18 Melpomene, and 19 Fortuna—showing significant extension and brightness variations up to a factor of two across the illuminated portion of the restored image. The diameters of the resolved asteroids are generally in good agreement with those in the TRIAD II file (E. F. Tedesco, 1989, In *Asteroids II* (Binzel, Gehrels, and Matthews, Eds.)). Diameters for 19 Fortuna and 624 Hektor (which are not in the TRIAD file) have been measured: 225 and 370 × 195 km, respectively.

Key Words: **asteroids; satellites.**

INTRODUCTION

Asteroids are generally believed to be the remnants of planetesimals that never accumulated into a planet. As a result, they provide some vital information about the protosolar nebula and the formation of planets. The main belt and Trojan asteroids appear to be in approximately their original orbits, thereby preserving information on the conditions in the protosolar nebula at the time and distance of their formation. In this respect, they are almost unique among the small bodies of the Solar System.

Imaging studies of asteroids at very high resolution can provide data on some important questions: Do asteroids today have satellites? How (if at all) did the parent bodies break up? If a satellite is present, what is the mass and density of the system? The presence or absence of satellites around asteroids would place constraints on the dynamical history of the original asteroidal bodies (e.g., Van Flandern *et al.* 1979, Weidenschilling *et al.* 1989).

By as early as 1979 there were already a number of far-reaching predictions in the literature (Hartmann 1979). In particular, various authors have suggested companions for the objects as listed in Table I. Such companions should be observable in high resolution images of asteroids.

0019-1035/99 $30.00

TABLE I
Suggested Companions

Asteroid	Primary asteroid diameter (km)	Satellite diameter (km)	Separation (km)	ΔM
9 Metis[a]	153	60	1100	2
18 Melpomene[b]	135	48	750	2.2
146 Lucina[c]	150	6	1600	7.0
216 Kleopatra[d]	$103 \times 82 \times 74$	$114 \times 60 \times 56$	221	0.2
532 Herculina[e]	220	50	1000	3.2
624 Hektor[f]	150×300	Contact binary?		
624 Hektor[c]	$110 \times 81 \times 74$	$111 \times 78 \times 70$	241	0.1

[a] Wang *et al.* (1981).
[b] Dunham (1979) (10 km topography).
[c] Arlot *et al.* (1985).
[d] Cellino *et al.* (1985).
[e] Binzel and Van Flandern (1979).
[f] Hartmann and Cruikshank (1978) (partially consolidated low-velocity collision product).

Most main belt asteroids (4 Vesta being an obvious exception) appear to have either undifferentiated surfaces or to be monolithic "chips off the old block" of a differentiated parent body. This observation implies that the parent bodies of the asteroids were undifferentiated or disrupted by fairly gentle collisions that shatter them along the interfaces between differentiated regions. On the other hand, the observation of variegated asteroidal surfaces would imply a more violent collisional history. This interpretation assumes that the asteroid does not become coated with an optically thick layer of material of uniform composition, such as dust or small, well mixed rock chips.

Many searches have been made for satellites of asteroids, but the only unambiguous detection has been that of Dactyl, the small satellite of 243 Ida, by the Galileo spacecraft (Belton *et al.* 1995). Theoretical considerations (e.g., Prokof'eva and Tarashchuk 1995) indicate that slower rotating asteroids should be more likely to keep companions than faster rotators. With a period of 4.65 h, however, 243 Ida does not fit into this class. The nondetection of satellites presented here indicates a problem with the conventional understanding of satellite formation and orbital evolution.

More recent analyses of the question of disruption of asteroids during collisions (e.g., Durda and Dermott 1997, Ryan and Melosh 1998) show that more small bodies are produced in catastrophic collisions than was previously thought, and with smaller velocities. Rather than breaking into a few large components, large (greater than 10 km diameter) rocky bodies are likely to shatter into a cloud of smaller particles, many with velocities too small to escape the gravitational potential of the original body. They will reaccrete into a "rubble pile," forming an asteroid with a homogeneous surface (and relaxed shape) despite the (potentially) differentiated origin of the material.

OBSERVATIONS

Two HST programs have surveyed 10 asteroids, in an attempt to image the illuminated portions of those bodies and to detect any possible companions. The first was program 4764, with principal investigator (PI) Ben Weiss, and the second program 4521, with PI Ben Zellner. Both programs used the uncorrected Wide-Field/Planetary Camera (WFPC1), and imaged the asteroids with the most sensitive CCD detector, PC6. The pixels are 0.043 arcs across. The *B* filter (F439W, centered at 4362 Å, FWHM 468 Å) was used for all objects in program 4764, and the *V* filter (F555W, centered at 5430 Å, FWHM 1600 Å) was used for 216 Kleopatra, 624 Hektor, and all of program 4521. The observations are summarized in Table II.

Program 4764 targeted five asteroids that were suspected—from either direct or occultation observations—of being binary systems. Information on predicted companions is summarized in Table I. Two pairs of images were made to allow for cosmic ray removal of two-filter observations. This tactic was later modified to use only one filter, with three images with longer exposure times and one with a shorter time.

TABLE II
Asteroid Observations

Asteroid	Observed (1993)	R	Δ	Phase (degrees)	Program	Filter(s)	Exp. time	Dataset name
9 Metis	17 Aug. 01:29	2.321	1.485	17	4521	F555W	2.0	w1k10r03
18 Melpomene	18 Jan. 09:20	2.220	1.255	9	4764	F439W	2.0	w1930104
19 Fortuna	10 Sept. 12:44	2.301	1.534	20	4521	F555W	5.0	w1k10i03
109 Felicitas	20 Nov. 07:01	1.938	1.131	23	4521	F555W	4.0	w1k10w03
146 Lucina	6 Oct. 09:34	2.889	2.062	13	4764	F439W	4.0	w1930204
216 Kleopatra	2 July 15:33	3.243	2.384	11	4764	F439W, F555W	7.0	w1930303
434 Hungaria	27 Nov. 14:12	1.955	1.243	26	4521	F555W	40	w1k10y03
532 Herculina	30 Sept. 08:42	3.216	2.387	12	4764	F439W	1.8	w1930404
624 Hektor	13 June 13:54	5.239	4.333	5	4764	F439, F555W	100 s	w1930504
674 Rachele	10 Sept. 16:33	2.715	1.962	16	4521	F555W	4.0	w1k10z03
674 Rachele	22 Nov. 02:30	2.578	1.712	14	4521	F555W	4.0	w1k11003

Program 4521 was more generally targeted, imaging bright, slowly rotating asteroids that reached opposition during April through December 1993. The primary intent was to search for companions, with a secondary emphasis on resolving the primary asteroid. This was a "snapshot" program for which exposures were scheduled when regular observations could not be fitted in the spacecraft calendar. Exposure times for this program were bracketed around the expected ideal, so the usual cosmic ray elimination routine could not be used with this data. Results from this program are based on the single best exposure, from which cosmic rays have been removed "by hand."

The snapshot observations were made under gyro control instead of the usual guidestar control. The pointing drift under gyro control is about 1 m per second. This means that the longest exposures (40 s, of 434 Hungaria) might have experienced a drift of up to one pixel during the time the shutter was open. As discussed below, 434 Hungaria appears point-like, there is no evidence of drift. Of the six observations made under gyro control, three match the TRIAD diameters exactly, two do not appear in the TRIAD file, and one (9 Metis) appears 13% larger than the TRIAD value. 9 Metis appears quite elongated and the difference is probably due to the particular aspect of the asteroid that was observed.

The HST images were subjected to the usual processing (correction of analog-to-digital conversion errors, bias subtraction, preflash correction, and flat-fielding) using the IRAF and STSDAS software, following the procedures in the *HST Data Handbook*. The time variation of the flat field was removed by multiplying each image by a "deltaflat." Finally, the unpaired images (from program 4521) were subjectively cleaned of cosmic ray strikes.

IMAGE RESTORATION

The aberrated point-spread function (psf) of the uncorrected HST+WFPC optics spreads a large amount of the light from a source over the surrounding area in the image. This scattered light can make it difficult to detect faint companion sources. Since any companion objects would appear extended (due to the size of the psf if not of the companion), we used iterative image restoration techniques to remove the aberrated light and to look for correlated groups of pixels.

We relied primarily on the maximum entropy (Gull and Daniell 1978, Wu 1994) method implemented in the STSDAS package, although the Lucy algorithm (Richardson 1972, and Lucy 1974) was used to corroborate the early results. These programs are iterative; that is, they compare an estimate of the unaberrated image convolved with the psf to the data and update the estimate based on the difference between the two. The programs require as input the degraded image, the psf, and a model for the noise. We used a theoretical psf calculated by the Tiny Tim software package (Krist 1993), although some early tests with observed psfs gave similar results. The Tiny Tim psf is preferred because it is noiseless and because it can be calculated at enhanced spatial sampling (discussed below). The WFPC1 has a "gain" of 8 electrons per data number, and a read noise of 13 electrons (*WFPC Instrument Handbook* V.2.1, p. 60). The maximum entropy program was run to convergence (often 50–60 iterations for point-like objects) or until the maximum number of iterations (200) was reached. The Lucy program was run for only 30 iterations. Further execution of either program did not improve the resulting image.

We ran several test procedures to determine how well these restoration techniques worked in the particular case of asteroids. While the restoration techniques are optimized for the usual astronomical cases of fields of point sources with or without background contributions with low spatial variation, images of asteroids have abrupt changes in brightness over small spatial scales, often with extended areas at the high signal level. In particular, we want to verify that image restoration will detect faint point sources near a well-exposed (possibly extended) source and that the size, shape, and brightness variations in such restorations can be trusted.

Figure 1 shows the results of such tests. The first two panels are a well-exposed (but not saturated) stellar image, before and after restoration. Note that 52% of the flux is contained in the four peak pixels of the restored image—an area of one quarter of an original Planetary Camera pixel. The third and fourth panels are the same PSF star to which has been added scaled down (by a factor of 10) and offset stellar images, before and after restoration. Note how the secondary images are barely visible in the raw image, but can be clearly seen (for most separations) in the restored image.

The last two panels of Fig. 1 show a model of extended sources of various sizes, and the result of convolving this model with a psf, adding noise, and restoring the degraded image. We find that a convolved image has a FWHM 15 to 25% broader than the model image and that after restoration the image had a FWHM 30% smaller than the original model at the small (1–5 pixel) sizes relevant here.

In addition to removing most of the wings of the psf, these restoration methods can increase the spatial sampling of high signal-to-noise data. A well-exposed WFPC1 image can often be restored at 4 times its original spatial sampling, subdividing each original pixel into 16 subpixels. All the asteroidal images are well exposed, to a level of 1/4 to 3/4 full well. Thus pixels on the asteroid have a signal-to-noise ratio (SNR) of 90 or better, so pixels in the restored images have a nominal SNR of at least five. The maximum entropy method with four times increased sampling was used for most of the results in this paper.

Figure 2 summarizes the result of the satellite detection simulations described above. The separation between the well-exposed parent object and the satellite point source (ΔS) is shown on the X axis, and the corresponding brightness difference at the detection limit (ΔM, in magnitudes) is shown on the Y axis. Thus satellites brighter than the detection limit will occupy the

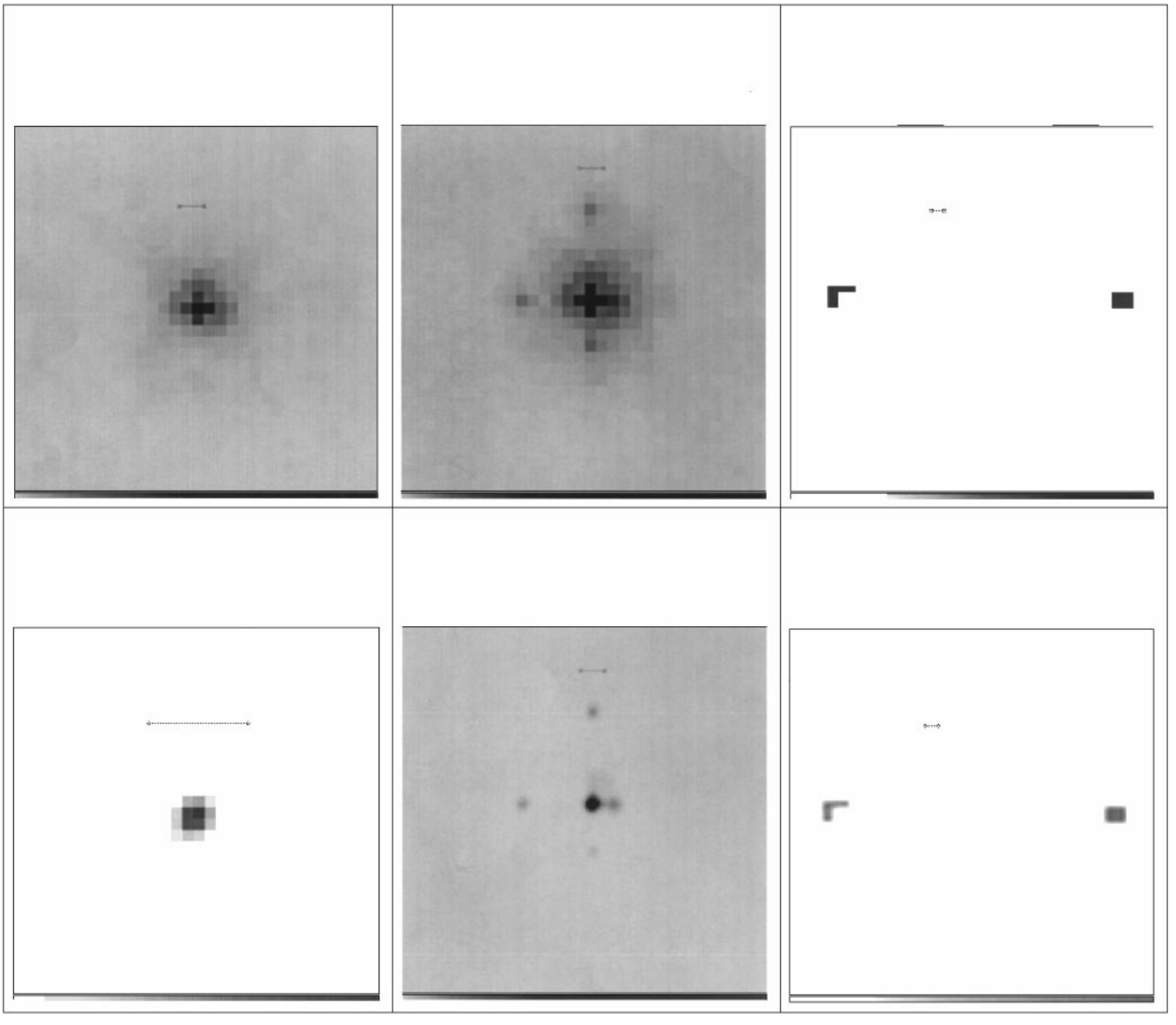

FIG. 1. Raw and restored PSF star and model images. Each scale bar is 0.1 inch long. (First column) A PSF star (top) and the maximum entropy reconstruction (bottom). (Second column) A PSF star with "companions" a factor of 10 fainter added to it (top) and the reconstruction (bottom). Note that the companions are nearly invisible in the raw image but easily detected in the reconstructed image. (Last column) A model of two extended sources (top) and the result of convolving this image with a point spread function, adding noise, and reconstructing the image (bottom). Note the brightness enhancements induced at the edges of the extended source. The FWHM of the reconstruction is 30% smaller than the original.

bottom part of the plot, while objects too faint to detect will be in the top part. A similar process for WFPC2 (PC chip) yields the results shown by the dashed line. The major gain is in the region of the first Airy ring: the correction for spherical aberration removes a significant amount of signal, and hence, noise in this area. A calculation based on the encircled energy for the (COSTAR-corrected) Faint Object Camera (FOC) (3000 s exposure, 1 ct/s on the primary object) is also shown. The FOC is sensitive mainly in the UV, however, and so is not a good instrument for detecting companions to red bodies reflecting light from a G-type star.

SIZE AND BRIGHTNESS

Table III compares the size and brightness of the observed bodies with those predicted in the literature. The diameters were determined by measuring the full width at half maximum (FWHM) of the asteroidal images before and after restoration. We measured the FWHM directly off of the profiles of the row and column going through the brightest part of the image. This FWHM measurement is good to 3%. If the (restored) image was obviously elongated, the image was rotated so that the long axis aligned with a row before the FWHM was measured. The

TABLE III
Asteroid Observations Results

Asteroid	Diameter (km) Raw	Diameter (km) Deconv.	Observed *V* magnitude	TRIAD *V*	TRIAD Diameter
9 Metis	200	235 × 165	9.67	9.83	174
18 Melpomene	155	150 × 125	8.80	9.12	148
19 Fortuna	210	225	11.03	10.89	??
109 Felicitas	100	90	11.91	11.70	91.6
146 Lucina	150	125	12.63	12.81	137
216 Kleopatra	225	270 × 110	12.14	12.58	140
434 Hungaria	70	55[a]	13.86	14.27	??
532 Herculina	230	195	10.76	10.43	231
624 Hektor	380 × 240	370 × 195	14.75	14.70	??
674 Rachele	145	100	11.80	11.84	101
674 Rachele	125	100	11.38	11.32	101

[a] Consistent with a point source.

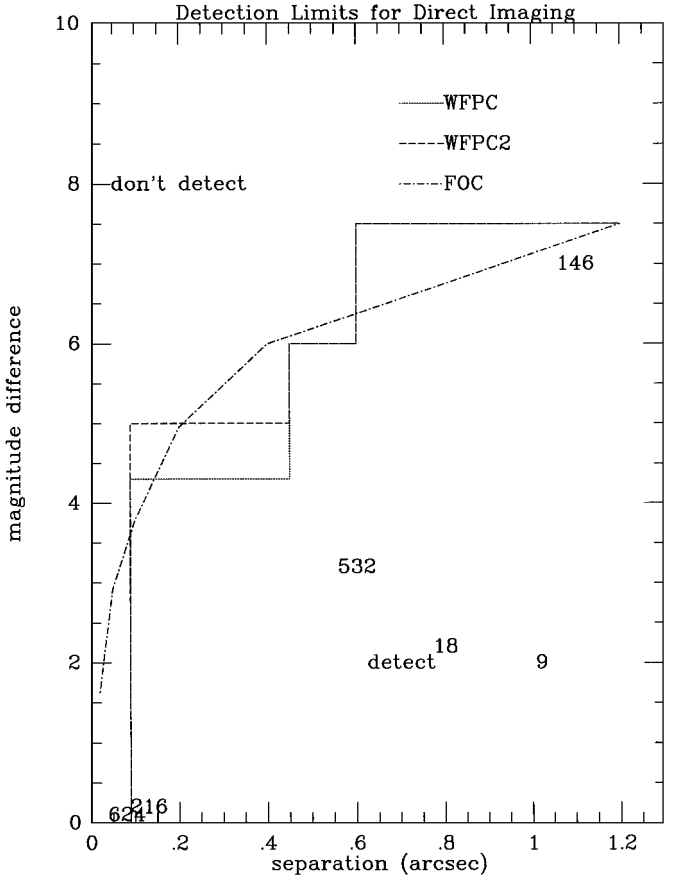

FIG. 2. Phase plot of detectability of secondary bodies in a well-exposed (but not saturated) image of a primary body. The closer a secondary body is to its primary in distance, the closer it must be in brightness to be detected. Only objects in the lower part of the plot can be detected. The dotted line shows the results for WFPC2—the main increase in detectability is in the intermediate region, 0.2 to 0.4 arcs from the primary image. The dot-dash line is a theoretical calculation for an FOC image with 3000 counts in the peak of the primary image. The numbers represent the separation in space and brightness for suggested companions (see Table I).

brightness of the asteroid was determined by measuring the count rate in the images before restoration, and correcting for background and instrumental effects as described in the *HST Data Handbook* (1995). Magnitudes in the *B* (F439W) passband were transformed to the *V* passband, assuming a G5 stellar spectrum.

The observed magnitudes show good agreement with the predictions of the TRIAD II file (Tedesco 1989) (see Table III). No attempt has been made to correct for the asteroidal lightcurves. The photometric process has an error of 5–10% (*HST Data Handbook* 1995). This serves primarily as a check of the HST photometric calibration, and of our reduction of the data.

The observed diameters (FWHM of the reconstructed images) are comparable to those determined by other sources. In all cases but one (434 Hungaria) the asteroids had larger FWHM than a stellar image reconstructed in a similar manner. We have corrected all the diameter measurements from restored images by a factor of 1.3 (see Image Restoration above). This factor brings the observed diameters into good agreement with those reported in the TRIAD file (see Table III).

Arlot *et al.* (1985) find a slightly smaller size for 146 Lucina than reported in the TRIAD file. This may account for the diameter measured in the restored image of this body being 9% lower than that given in the TRIAD file.

SEARCH FOR COMPANIONS

No companions were visible in any of the raw images. However, fainter satellites might be hidden in the Airy disc and diffraction spikes, enhanced by the spherical aberration of the HST primary mirror. To reduce this signal, the deepest unsaturated images of each asteroid were subjected to both the maximum entropy and Lucy restoration programs. These programs yielded similar results: even after restoration, no companions were visible. This result means that either (a) no companions actually exist, (b) companions exist but are too faint and/or too close to the main asteroid to be resolved, or (c) the imperfections in the instrument or restoration process prevented detection of objects that would otherwise have been visible.

Figure 2 shows the positions of satellite "detections" from the literature as asteroid numbers in the plot. Any pair of objects (parent and satellite) with the characteristic coordinates (magnitude difference ΔM, and projected separation ΔS) falling in the top region of the plot cannot be observed in well exposed WFPC1 images, even after restoration. Conversely, all satellites with coordinates located in the bottom region at the time of observation should be observable (except in the rare case of the satellite being in conjunction with the parent). For example, Table I shows a prediction of a 60-km diameter to 9 Metis, with a 1100-km separation. This corresponds to $\Delta M = 2$ and $\Delta S = 1$" at the time of observation. This is represented as the number "9" in Fig. 2. Such a companion should be easily seen in our data.

Because the WFPC2 phase space resembles that of WFPC1 except in the region ΔS between 0.2 and 0.4 arcs, we can

reasonably eliminate case (c) (above). That is, we conclude that if any satellites of the observed asteroids exist in these regions at the time of the observations, then those satellites are undetected because of faintness or projected proximity to the main asteroid.

Figure 2 shows that:

(1) We should have detected multiplicity in asteroids 9, 18, and 532 if their characteristic geometries were accurately predicted. Our nondetection of companions suggests that either these predictions are inaccurate (the companion is either not present, or is significantly smaller than reported or darker than the primary) or we were unlucky and the satellite appeared too near the primary asteroid at the time of observation to be distinguished.

(2) Detection of multiplicity in asteroids 146, 216, and 624 would be marginal given their predicted geometries. Thus we can neither verify nor negate these predictions. These asteroids were imaged in the hopes that there might be more satellites farther from the primary than had been reported, or that the reported companions might have been observed in a close approach to the primary on an eccentric orbit. Note that both 216 Kleopatra and 624 Hektor appear quite elongated, however (see Fig. 3).

(3) Future attempts with WFPC2 may be able to resolve large outer satellites for 216 and 624. The dotted line in Fig. 2 shows the $\Delta M/\Delta S$ line for the WFPC2, determined in the same way as for the WFPC1. The main improvement in detectability is in the intermediate range—very close to the primary, the core of the PSF (largely unaberrated even in the WFPC1) limits the process, while at larger distances the low signal of the satellite image (limited by the dynamic range of the analog to digital converter) is the limiting factor. Note that if the image of the primary is saturated, a fainter companion may be detected, but image restoration becomes problematical. The dot-dash line in Fig. 2 shows the theoretical limits of the FOC, with 3000 counts in the primary image.

RESOLVED BODIES

All of the asteroids except 434 Hungaria had broader FWHM in their restored images than would be expected in the restored image of a point source. Three showed clear disks (Fig. 3): 9 Metis, 18 Melpomene, and 19 Fortuna. Care should be taken in the interpretation of individual features in the restored images, as discussed at the end of this section.

9 Metis appears oblong, with a long axis of 235 km and a short axis of 165 km. This is 13% larger than the 174-km diameter determined by Kissling *et al.* (1991) and is more elongated than the 1.27 axis ratio reported by Drummond *et al.* (1991). The shape appears irregular, with several brightness enhancements along the limb.

18 Melpomene is less elongated, about 150 by 125 km, in good agreement with the 135-km size reported by Dunham (1979). The brightness enhancements on the sunward and antisunward ends of the image probably reflect the effect of the asteroid's shape on the image restoration process, rather than any variation in surface properties.

19 Fortuna appears nearly circular, 225 km in diameter. The slight elongation is in good agreement with the minimum axis ratio of 0.93, from Drummond *et al.* (1991). The brightness enhancement in the sunward direction is not balanced by one on the terminator side of the disk.

Note that bright spots at the edge of the disk in a restored image are common, both in the data and in simulations of the restored images. In the simulations (compare the last two panels of Fig. 1), these enhancements are due to the restoration algorithm overcompensating for the large brightness gradient at the limb of the model. There are no features in the restored images that cannot be explained by the restoration process overcompensating for the sharp limb of the body.

The resolved observations were made at moderate phase angles: 17° for 9 Metis, 9° for 18 Melpomene, and 20° for 19 Fortuna. 18 Melpomene was observed at about half the phase angle of the other two asteroids and has about half the contrast between the brightest spot and the disk center in the restored image than is seen in the other two asteroids. This observation is suggestive that at least part of the brightness variation across the disk may be real. If so, it is probably due to the greater contrast between dark space and the sunlit limb of the asteroid compared to the contrast between the terminator limb and space—the greater the contrast, the greater the enhancement.

The lack of images in other wavelength bands (the purpose of the programs was primarily a satellite search) does not allow a mineralogical interpretation like that of Binzel *et al.* (1997). We note however, that similar restorations of HST images of 4 Vesta showed similar brightness enhancements on the sunward limb (Zellner *et al.* 1997). This enhancement was about 30%, and the observations were made at a phase angle of 11°. This supports the trend of increasing brightness enhancement with increasing phase. Note that while the bright spots reported in this paper can usually be minimized by adding a constant to the input image before the restoration process, the sunward brightness gradient in the images of 4 Vesta cannot be eliminated in this manner. The spatial resolution and disk size of the 4 Vesta dataset are much better than that of the asteroids reported in this paper.

The small extent of the resolved images, as well as the ambiguity introduced in the restoration process by the bright spots along the limb, make it impossible to determine if there are any albedo features on these asteroids and so renders a determination of surface heterogeneity difficult. The azimuthal nonuniformity of the brightness enhancement is due to the interaction between the shape of the asteroid and the observation and reconstruction process and not to any compositional variation.

Note that, while not necessarily showing a definite disk, 216 Kleopatra and 624 Hektor show axial ratios of around a factor of two. This is in keeping with the suggestions of Hartmann and Cruikshank (1978), Arlot *et al.* (1985), and Cellino *et al.* (1985) that these objects may be contact or near-contact binaries. At the time of these observations, the two bodies (if present)

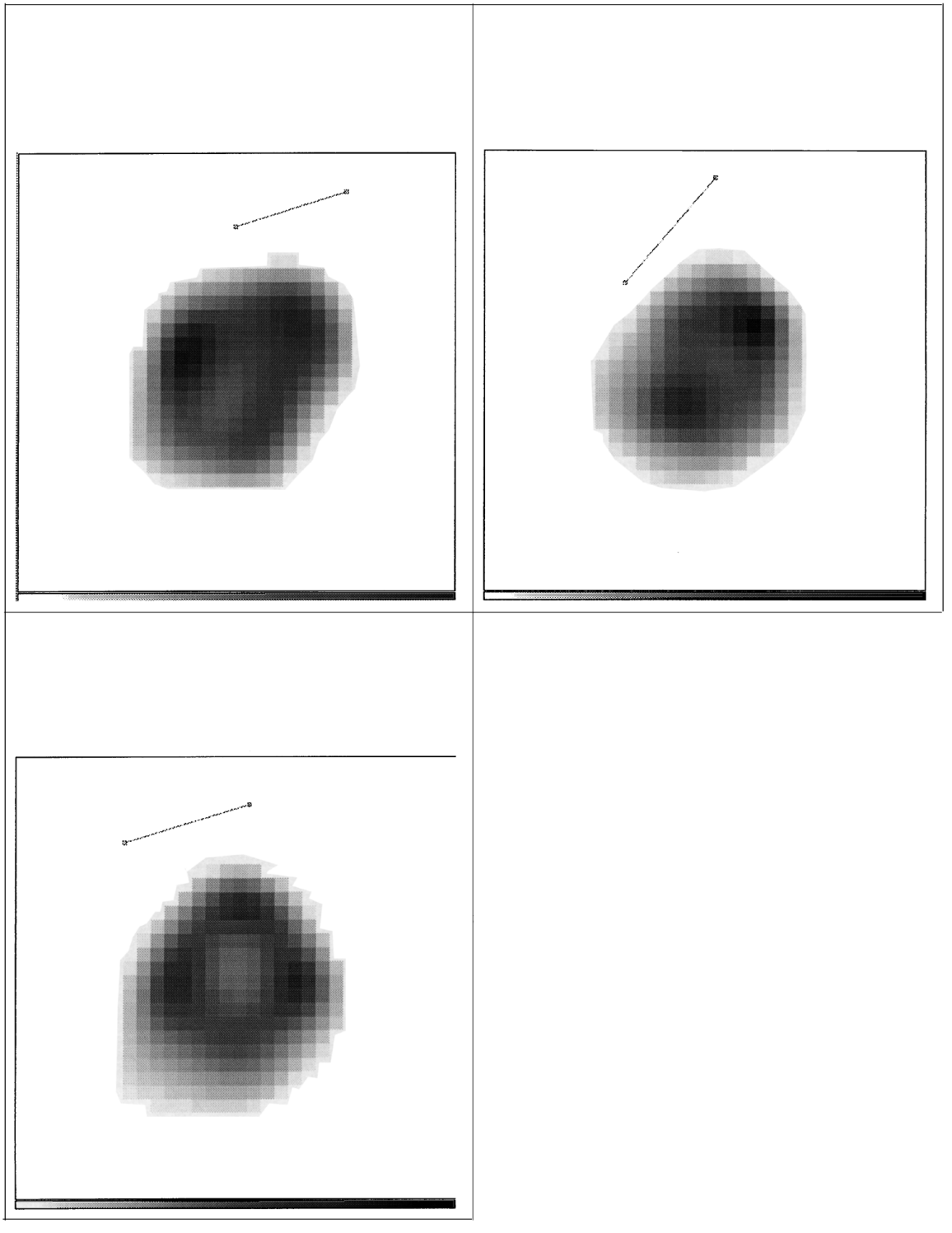

FIG. 3. Restored images of 9 Metis (top left), 18 Melpomene (top right), and 19 Fortuna (bottom). The asteroids all show resolved "disks" after restoration, with bright points primarily on the sunward (upper) limb. No other albedo features are reliably determined. The scale bars are all 0.1 inch long and point to celestial north from the vertical centerline of the images.

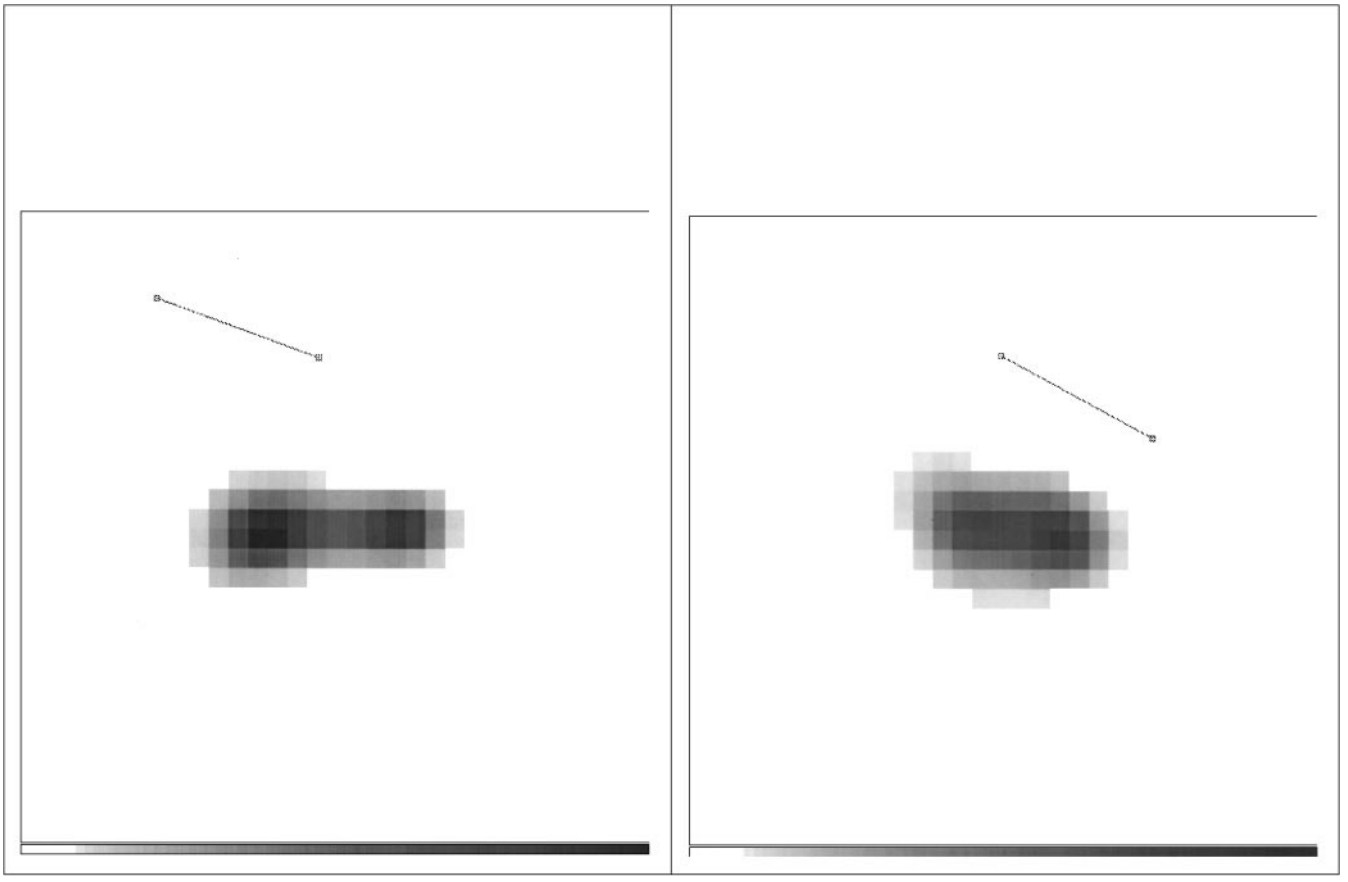

FIG. 4. Restored images of 216 Kleopatra (left) and 624 Hektor (right). Although suggested companions or binary nature (see Table I) cannot be confirmed, the elongated appearance does not rule out a contact binary nature for these asteroids. Note that the brightness enhancements at the ends of the reconstruction of 216 Kleopatra are consistent with artifacts induced in the image reconstruction (Conclusions). The scale bars are all 0.1 inch long and point to celestial north from the vertical centerline of the images.

could not be unequivocally distinguished. Figure 4 shows maximum entropy restorations of images of these objects. Note that although 216 Kleopatra appears to be two bodies with a brightness dip between them, the ends of the asteroid's image are enhanced by a factor of two over the middle. This enhancement is easily explained by the effects of the image restoration discussed above—these observations are unable to distinguish between a very elongated asteroid, a contact binary, or two bodies in close orbit, for 216 Kleopatra. 624 Hektor is not quite so elongated, and does not show brightness enhancements at its ends—it is probably one body.

CONCLUSIONS

No companion bodies were found in images of 10 asteroids (674 Rachele was observed twice). The upper limits for these nondetections are significant compared to previous suggestions of companions for all but three asteroids (146 Lucina, 216 Kleopatra, and 624 Hektor).

All asteroids except 434 Hungaria have larger FWHM than point sources observed in a similar manner. Simulations of the convolution and restoration processes indicate that the sizes of restored images are about 30% smaller than the original model sizes. After correction for this factor, the sizes and axial ratios of the asteroids observed here agree satisfactorily with values in the literature.

Image restoration of three best resolved asteroids show brightness enhancements generally on their sunward limbs of 50 to 100% over disk center. The brightness enhancements are probably due to the image restoration process. This effect is much larger than any possible albedo features, and no such features (other than these limb enhancements) are seen in the restorations. Thus no constraint on the surface heterogeneity can be made from this data.

ACKNOWLEDGMENTS

ADS wishes to thank Clark Chapman and an anonymous referee for excellent suggestions and references. Based on observations with the NASA/ESA Hubble Space Telescope, obtained at the Space Telescope Science Institute, which is operated by the Association of Universities for Research in Astronomy, Inc., under NASA Contract NAS5-26555.

REFERENCES

Arlot, J. E., J. Lecacheux, C. Richardson, and W. Thuillot 1985. A possible satellite of 146 Lucina. *Icarus* **61**, 224–231.

Belton, M. J. S., B. E. A. Mueller, L. D'Amario, D. Byrnes, K. P. Klaasen, P. C. Thomas, J. Veverka, Harch, M. E. Davies, W. Merline, C. R. Chapman, D. Davis, T. Denk, J.-M. Petit, R. Greenberg, A. McEwen, A. Storrs, and B. Zellner 1995. The discovery and orbit of 1993 (243)1 Dactyl. *Icarus* **120**, 185–199.

Binzel, R. P., and T. Van Flandern 1979. Minor planets: The discovery of minor satellites. *Science* **203**, 903–905.

Binzel, R. P., M. J. Gaffey, P. Thomas, B. Zellner, A. Storrs, and E. Wells 1997. Geologic mapping of Vesta from 1994 Hubble Space Telescope images. *Icarus* **128**, 95–103.

Cellino, A., R. Pannunzio, V. Zappalà, P. Farinella, and P. Paolicchi 1985. Do we observe light curves of binary asteroids? *Astron. Astrophys.* **144**, 355–362.

Drummond, J. D., S. J. Weidenschilling, C. R. Chapman, and D. R. Davis 1991. Photometric geodesy of main-belt asteroids. *Icarus* **89**, 44–64.

Dunham, D. 1979. Duplicity of both 18 Melpomene and SAO114159 discovered during occultation. *Occult. Newsl.* **2**(2), 12–16.

Durda, D. D., and S. F. Dermott 1997. The collisional evolution of the asteroid belt and its contribution to the Zodical cloud. *Icarus* **130**, 140–164.

Gull, S. F., and G. J. Daniell 1978. Image reconstruction from incomplete and noisy data. *Nature* **272**, 686–690.

Hartmann, W. K. 1979. Diverse puzzling asteroids and a possible unified explanation. In *Asteroids* (T. Gehrels, Ed.), pp. 466–479. Univ. of Arizona Press, Tucson.

Hartmann, W. K., and D. Cruikshank 1978. The nature of Trojan asteroid 624 Hektor. *Icarus* **36**, 353–366.

Kissling, W. M., G. L. Blow, W. H. Allen, J. Priestley, P. Riley, P. Daalder, and M. George 1991. The diameter of (9) Metis from the occultation of SAO 190531. *Proc. ASA* **9**(1), 150–152.

Krist, J. 1993. *The Tiny Tim User's Manual*. Space Telescope Science Institute.

Lucy, L. B. 1974. An iterative technique for the rectification of observed distributions. *Astrophys. J.* **79**, 745–754.

Prokof'eva, V. V., and Tarashchuk, V. P. 1995. Development of binary asteroids concepts. *Solar Syst. Res.* **29**, 123–132.

Richardson, W. H. 1972. Bayesian-based iterative method of image restoration, *J. Opt. Soc. Am.* **62**, 55–59.

Ryan, E. V., and H. J. Melosh 1998. Impact fragmentation: From the laboratory to asteroids. *Icarus* **133**, 1–24.

Tedesco, E. F. 1989. Asteroid magnitudes, UBV colors, and IRAS albedos and diameters. In *Asteroids II* (R. P. Binzel, T. Gehrels, and M. S. Matthews, Eds.), pp. 1090–1138. Univ. of Arizona Press, Tucson.

Van Flandern, T. C., E. F. Tedesco, and R. P. Binzel 1979. Satellites of asteroids. In *Asteroids* (T. Gehrels, Ed.), pp. 443–465. Univ. of Arizona Press, Tucson.

Wang Sichao, Wu Yuezhen, Bao Mengxian, Deng Liwu, and Wu Sufang 1981. A possible satellite of 9 Metis. *Icarus* **46**, 285–287.

Weidenschilling, S. J., P. Paolicchi, and V. Zappala, 1989. Do asteroids have satellites? In *Asteroids II* (R. P. Binzel, T. Gehrels, and M. S. Matthews, Eds.), pp. 643–658. Univ. of Arizona Press, Tucson.

Wu, N. 1994. Model updating in the MEM algorithm. In *The Restoration of HST Images and Spectra* (Hanisch and White, Eds.), pp. 58–63. Space Telescope Science Inst., Baltimore, MD.

Zellner, B., R. Albrecht, R. P. Binzel, M. J. Gaffey, P. Thomas, A. Storrs, and E. Wells 1997. Hubble Space Telescope images of Asteroid 4 Vesta. *Icarus* **128**, 83–87.